Journal of Fluorescence, Vol. 13, No. 3, May 2003 (© 2003)

Effects of the Solvent Refractive Index and Its Dispersion on the Radiative Decay Rate and Extinction Coefficient of a Fluorescent Solute

Dmitri Toptygin[1]

Received August 28, 2002; revised December 4, 2002; accepted December 7, 2002

It is well known that the probabilities of radiative transitions in a medium differ from those in vacuum. Excitation of a fluorescent molecule and its radiative decay are examples of radiative transitions. The rates of these processes in solution depend on the optical characteristics of the solvent. In this article the radiative decay rate and the extinction coefficient of a fluorescent molecule in solution are expressed in terms of the intrinsic properties of the fluorescent molecule (electronic transition moments) and the optical characteristics of the solvent (refractive index, group velocity of light). It is shown that the group velocity does not enter in the final expressions for the radiative decay rate and the extinction coefficient; this means that the dispersion of the refractive index has no effect on these quantities. The expressions for both the radiative decay rate and the extinction coefficient contain the refractive index of the solvent and the local field correction factor. The latter depends on the cavity model, and, for some cavity models, on the shape of the cavity. Four types of cavity models are discussed; for each model the limits of applicability are examined. Experimental evidence in support of specific cavity models is reviewed.

KEY WORDS: Radiative decay rate; extinction coefficient; refractive index; local field correction; empty cavity model.

INTRODUCTION

It is well known that the quantum yield (η) and the lifetime (τ) of an electronically excited fluorescent molecule in a transparent host medium are determined by the radiative decay rate (k_r) and the nonradiative decay rate (k_{nr}) [1]:

$$\eta = \frac{k_r}{k_r + k_{nr}} \tag{1}$$

$$\tau = \frac{1}{k_r + k_{nr}} \tag{2}$$

It is also well known that the nonradiative decay rate varies with temperature and can be significantly increased by the addition of quenchers, such as molecular oxygen. The radiative decay rate is often believed to be invariant and immutable. The reciprocal of the radiative decay rate is called the natural lifetime [1],

$$\tau_0 = \frac{1}{k_r} \tag{3}$$

The term *natural lifetime* may create a false impression that this is an intrinsic property of the fluorescent molecule. However, the truth is that radiative decay results from coupling between the excited molecule and optical-frequency electromagnetic waves (light waves). The characteristics of these waves depend on the optical properties of the molecule's environment, and so do the radiative decay rate and the natural lifetime. Only in free space (i.e., in vacuum) does the natural

[1]Department of Biology, Johns Hopkins University, 3400 North Charles Street, Baltimore, Maryland 21218. E-mail: toptygin@jhu.edu

1053-0509/03/0500-0201/0

lifetime depend on nothing but the intrinsic properties of the fluorescent molecule.

The refractive index is defined as the ratio of the phase velocity of monochrome light waves in vacuum to that in the medium and represents the most important optical property of any transparent homogeneous isotropic medium, such as a regular solvent. The refractive index effect on the radiative decay rate should not be confused with the solvatochromic effect (solvent-dependent spectral shifts of absorption and emission bands). The physical mechanism of the solvatochromic effect have been studied in great detail by Ooshika, Mataga, Kaifu, Koizumi, McRae, Lippert, and Bakhshiev [2–6]. By coincidence, the refractive index also enters in the expressions for solvatochromic spectral shifts. Apart form this coincidence, there is nothing in common between the solvatochromic effect and the refractive index effect discussed in this article.

Indications that the radiative decay rate depends on the refractive index of the host medium can be found in scientific papers printed over 75 years ago. In 1926 Perrin published a formula that involved both the radiative decay rate and the refractive index [7]. In a footnote, Perrin wrote that the formula had been used by different authors, but he did not specify who obtained it first. Here is the formula in its original form:

$$\frac{1}{\tau_0} = \frac{8\pi n^2}{c^2}\,\nu_m^2 \frac{1}{N}\int \alpha(\nu)\,d\nu \qquad (4)$$

Here $1/\tau_o$ represents the radiative decay rate, n is the refractive index of the host medium, c is the speed of light in vacuum, ν_m is the mean frequency of fluorescence emission, N is the number of fluorescent molecules per unit volume, $\alpha(\nu)$ is the absorption coefficient at a frequency ν, and the integration is carried out over the entire absorption band that corresponds to the lowest excited singlet electronic state. Eq. (4) can be easily converted from the absorption coefficient to the decadic molar extinction coefficient:

$$\frac{1}{\tau_0} = \frac{8\pi n^2}{c^2}\,\nu_m^2 \frac{\ln(10)}{N_A}\int \varepsilon(\nu)\,d\nu \qquad (5)$$

Here ln(10) is the natural logarithm of 10, N_A is Avogadro's number, $\varepsilon(\nu)$ is the decadic molar extinction coefficient at a frequency ν, and all other quantities are the same as in Eq. (4).

Note that Eq. (5) relates the radiative decay rate of a fluorescent molecule to its extinction coefficient spectrum. This equation is not very accurate, especially in the case of fluorescent molecules with large Stokes shifts. In 1962 Strickler and Berg came up with a more accurate relationship [8]:

$$\frac{1}{\tau_0} = \frac{8\pi n^2}{c^2}\,\langle \nu_f^{-3}\rangle_{Av}^{-1} \frac{\ln(10)}{N_A}\int \frac{\varepsilon(\nu)}{\nu}\,d\nu \qquad (6)$$

In Eq. (6) ν_f is a frequency of fluorescence emission, and a precise definition of the mean value $\langle \nu_f^{-3}\rangle_{Av}^{-1}$ will be given later; see the note after Eq. (36).

Strickler and Berg's equation has been widely used to obtain theoretical estimates of radiative decay rates, and for this purpose it is perfectly suitable. It is necessary to emphasize, however, that this equation does not express the radiative decay rate in terms of intrinsic properties of a fluorescent molecule. The extinction coefficient is not an intrinsic property of a fluorescent molecule. Eqs. (5, 6) say nothing about whether $1/\tau_0$ or ε or both vary with n. If ε was n–invariant, then $1/\tau_0$ would be directly proportional to n^2. However, if $1/\tau_0$ was n–invariant, then ε would be inversely proportional to n^2. In reality, however, both the radiative decay rate and the extinction coefficient vary with the refractive index. The laws describing the refractive index variation of $1/\tau_0$ and ε can be obtained by expressing both $1/\tau_0$ and ε in terms of an intrinsic property of the fluorescent molecule rather than in terms of each other.

The intrinsic property of a fluorescent molecule responsible for its emission is the electric transition dipole moment $\vec{\mu}_{01}$; for a definition, see the section about static and transition dipole moments. An expression in terms of $|\vec{\mu}_{01}|^2$ for the radiative decay rate (known among physicists as the spontaneous emission rate) can be found in numerous textbooks on quantum electrodynamics and quantum mechanics. Unfortunately, most of these textbooks consider spontaneous emission in vacuum, and the expressions obtained there are inapplicable to the case of a fluorescent molecule in solution.

Expressions in terms of $|\vec{\mu}_{01}|^2$ for the radiative decay rate of a fluorescent molecule in a medium can be found in recent physical literature. Different expressions have been derived for different physical models of the cavity containing the fluorescent molecule. The fluorescent molecule and the host medium cannot occupy the same volume; thus one can always say that the fluorescent molecule is located in a cavity inside the host medium. The shape of the cavity is usually thought to be spherical, but it does not have to be spherical in all cases. The host medium outside the cavity is usually treated as a classical homogeneous dielectric. The boundary conditions at the cavity surface depend on whether the material inside the cavity is believed to be the same as the host medium or the same as vacuum; this results in two different kinds

of models: the virtual cavity models and the empty cavity models. The expression for the radiative decay rate depends on the kind of model and on the shape of the cavity. Different cavity kinds and shapes will be reviewed later in this article in the order of increasing complexity. Before this can be done, the basic concepts will be defined in the following section, which is self-contained, so that a scientist unfamiliar with quantum mechanics and quantum electrodynamics should be able to understand the logic of all the statements.

DEFINITION OF BASIC CONCEPTS

Static and Transition Electric Dipole Moments

Electromagnetic waves couple with dipole, quadrupole, and higher multipole moments of any system that emits or absorbs electromagnetic radiation [9]. A cellular telephone and a fluorescent molecule are two common examples of such systems. If the linear dimensions of a system are much smaller than the wavelength (which is true for all fluorescent molecules), then the dipole coupling is much stronger than the quadrupole and higher multipole couplings [9,10]. Also, the coupling of electric moments with electromagnetic waves is much stronger than that of magnetic moments [9,10]. For this reason, all magnetic moments, as well as electric quadrupole and higher multipole moments, can be neglected if a fluorescent molecule has a nonzero electric dipole moment. Accurate expressions for the radiative decay rates and extinction coefficients can be obtained by considering the coupling of just electric dipole moments with electromagnetic waves. Exceptions from this rule are some fluorescent metal ions with zero electric dipole moments.

In classical (nonquantum) mechanics the electric dipole moment of a system of charged particles is defined as a sum over all particles of the products of each particle's charge and radius-vector [9]:

$$\vec{\mu} = \sum_m q_m \vec{r}_m \tag{7}$$

Here m is the number of a particle, q_m is its charge, and $\vec{r}_m$ is its radius-vector (a radius-vector can be thought of as a set of three numbers x_m, y_m, z_m that represent the coordinates of the particle). A typical fluorescent molecule consists of a number of charged particles: positively charged nuclei and negatively charged electrons. For example, *p*-terphenyl (1,4–diphenyl benzene), a small fluorescent molecule with a very high radiative decay rate, consists of 154 particles: 32 nuclei and 122 electrons. For *p*-terphenyl and many other rigid molecules it is fair to use the fixed-nuclei approximation, that is, the approximation in which the coordinates of all the nuclei have specific values. This approach would never work for electrons, which are always "fuzzy," and therefore their coordinates do not have specific values. This makes it impossible to calculate the dipole moment of a fluorescent molecule in the framework of classical mechanics.

In quantum mechanics the state of a molecule is described by its wavefunction Ψ [11]. In the fixed-nuclei approximation the wavefunction is a function of the coordinates of all the electrons. Wavefunctions of stationary states are of special significance for three reasons: (i) stationary states do not change with time; (ii) when a molecule is in a stationary state, it has a definite value of energy E; and (iii) an arbitrary wavefunction can be represented as a linear combination of the wavefunctions of the stationary states [11]. Each stationary state is completely characterized by its wavefunction Ψ_i and energy E_i. It is convenient to number all singlet stationary states of a molecule in the order of ascending energy, $E_0 < E_1 < E_2 < \ldots$. All electric dipole moments of a molecule can be defined in terms of its stationary-state wavefunctions [11]:

$$\vec{\mu}_{ji} = \int\int\ldots\int \Psi_j^* \, \vec{\mu} \, \Psi_i \, dx_1 \, dy_1 \, dz_1 \ldots dx_m \, dy_m \, dz_m \ldots \tag{8}$$

Here Ψ_j^* is the complex conjugate wavefunction of stationary state j, Ψ_i is the wavefunction of stationary state i, $\vec{\mu}$ is defined in Eq. (7), and the integration is carried out over every coordinate of every electron (here electron coordinates play the roles of integration variables rather than the numbers that define a specific location of the electron).

Because the dipole moment on the left side of Eq. (8) has two indexes: j and i, Eq. (8) actually defines the elements of a matrix known as the matrix of the electric dipole moment. The diagonal matrix elements (the elements with $j = i$) represent static dipole moments of the molecule in different stationary states. For example, $\vec{\mu}_{00}$ is the static (permanent) dipole moment of the molecule in its ground state ($i = 0$). If the molecule is nonpolar, then $\vec{\mu}_{00} = 0$. For a polar molecule $\vec{\mu}_{00} \neq 0$. The static dipole moment $\vec{\mu}_{11}$ of the lowest singlet excited state ($i = 1$) may differ from that of the ground state. If $\vec{\mu}_{11} \neq \vec{\mu}_{00}$, then the absorption spectrum and the fluorescence emission spectrum of the molecule vary with the solvent polarity; such molecule is called solvatochromic. If $\vec{\mu}_{11} = \vec{\mu}_{00}$, then the molecule is not solvatochromic.

Unlike the diagonal matrix elements, which are all static, every off-diagonal matrix element $\vec{\mu}_{ji}$ ($j \neq i$) oscillates at a frequency [11]:

$$\omega_{ji} = \frac{E_j - E_i}{\hbar} \tag{9}$$

and can couple only with an electromagnetic wave that has the same frequency (note, that the circular frequencies denoted by ω are 2π times greater than the cyclic frequencies denoted by ν). In Eq. (9) $\hbar$ is Planck's constant divided by 2π, and ω_{ji} is called the transition frequency between the stationary state i and the stationary state j [11]. The corresponding off-diagonal matrix element $\vec{\mu}_{ji}$ is called the transition dipole moment between the stationary state i and the stationary state j. For any matrix element the last index (i) always corresponds to the initial state, and the first index (j) corresponds to the final state. The probability of a radiative transition $j \leftarrow i$ is determined by the moment $\vec{\mu}_{ji}$ and by the characteristics of electromagnetic waves. All transition dipole moments represent intrinsic properties of the fluorescent molecule, which follows directly from their definition in Eq. (8). The radiative decay rate is essentially the rate of radiative transition $0 \leftarrow 1$, therefore it is determined by $\vec{\mu}_{10}$. The extinction coefficient for the lowest-energy absorption band (transition $1 \leftarrow 0$) is determined by $\vec{\mu}_{10}$. From the fundamental properties of Hermitian operators [11] it follows that the squared magnitudes of both transition moments are equal:

$$|\vec{\mu}_{10}|^2 = |\vec{\mu}_{01}|^2 \tag{10}$$

This fundamental relationship between the off-diagonal matrix elements responsible for the absorption and emission is in the basis of the relationships in Eqs. (4–6). There are no relationships between off-diagonal and diagonal matrix elements; therefore the ability of a molecule to absorb and emit light has nothing to do with its polarity or solvatochromism. For example, benzene is nonpolar, nonsolvatochromic, its extinction coefficient and radiative decay rate are low. *p*-Terphenyl is also nonpolar and nonsolvatochromic, but its extinction coefficient and radiative decay rate are high. Coumarine is polar, solvatochromic, its extinction coefficient and radiative decay rate are high. Phenol is also polar and slightly solvatochromic, but its extinction coefficient and radiative decay rate are low.

Electromagnetic Field Oscillators

Fluorescent molecules absorb and emit photons. Photons are strictly defined in quantum electrodynamics, and the definition is based on the concept of electromagnetic field oscillators [12]. Probabilities of absorption and emission depend on the amplitudes of electric field oscillations. The probability of emission is also directly proportional to the density of field oscillators on the energy scale. In unlimited space the density is infinite, which makes it difficult to calculate the probabilities of radiative transitions. The problem is usually resolved by confining electromagnetic radiation to a box of a finite volume V. The actual value of V is not important, because it always cancels out in expressions for transition probabilities. The only limitation on the dimensions of the box arise from the condition that the closest wall of the box must be more than $1/(2\Delta\overline{\nu})$ away from the fluorescent molecule, where $\Delta\overline{\nu}$ denotes the width of the corresponding absorption or emission spectrum on the wavenumber scale (for details see the discussion of distance cutoff for medium effects). For a typical fluorescent molecule $1/(2\Delta\overline{\nu})$ is of the order of 1 μm; therefore the smallest box can be as small as about 10 μm × 10 μm × 10 μm. There is no upper limit on the size of the box. The number of field oscillators with frequencies not exceeding ω in the box will be denoted N_ω. If the box contains one homogeneous isotropic transparent medium of a refractive index n, then

$$N_\omega = \frac{Vn^3\omega^3}{3\pi^2c^3} \tag{11}$$

The density of field oscillators per unit energy is defined as the derivative of N_ω with respect to photon energy:

$$\rho(\omega) = \frac{\partial N_\omega}{\partial \hbar\omega} \tag{12}$$

While taking the derivative, it is important to take into account the frequency dispersion of the refractive index; this yields

$$\rho(\omega) = \frac{Vn^2\omega^2}{\pi^2\hbar c^2 u} \tag{13}$$

Here u denotes the group velocity of light waves in the medium [13],

$$u = c\left(n + \omega\frac{\partial n}{\partial \omega}\right)^{-1} \tag{14}$$

Eq. (13) gives the density of field oscillators in any isotropic homogeneous transparent medium of macroscopic dimensions. Regular transparent liquids, such as water or cyclohexane, satisfy all these requirements. The presence of microscopic foreign particles, such as fluorescent molecules, protein molecules, small vesicles, or microscopic metal particles, has little effect on the field

oscillator density if the total volume occupied by these particles is very small as compared to V, the volume of the box. If two or more media of macroscopic dimensions, for example, a microscope cover glass and immersion medium, fill the box, then Eq. (13) can be applied to the partial volumes occupied by different media, and then the results can be added up.

Unlike the density of field oscillators, which is a property of the entire box, and therefore has the same value at every point inside the box, the amplitude of electric field oscillations is not expected to be the same at every point inside the box [14,15]. If the box contains an interface between two media, then the waves reflected off the interface interfere with the incident waves, which produces a spatial variation in the amplitude of electric field oscillations. However, if the box contains no interfaces and cyclic boundary conditions are chosen, then the macroscopic electric field has a constant oscillation amplitude everywhere inside the box. The constant amplitude results in simple derivation of expressions for the probabilities of radiative transitions. Although the final expressions for these probabilities are independent of the choice of the box dimensions and boundary conditions, one can certainly benefit from the simplification of the intermediate steps. This can be achieved by excluding all interfaces from the box. For example, consider a fluorescent molecule separated by 1 mm from a cuvette wall. If a 3 mm $\times$ 3 mm $\times$ 3 mm box centered at the molecule is chosen, then the interface between the solvent and the cuvette wall material will be inside the box. Choosing a 1 mm $\times$ 1 mm $\times$ 1 mm box centered at the molecule eliminates this inessential interface and realizes the desired simplification. However, if the distance from the cuvette wall was 0.1 μm rather than 1 mm, then this trick would not work, because every wall of the box must be more than $1/(2\Delta\overline{\nu})$ away from the fluorescent molecule, for details see the discussion of distance cutoff for medium effects.

If the box contains no interfaces and the amplitude of macroscopic electric field oscillations is constant, then the amplitude can be expressed from simple normalization conditions. The normalization conditions are different in the case of spontaneous emission and in the case of induced transitions, such as absorption and stimulated emission. In the case of spontaneous emission the amplitude must be normalized to one photon in the box:

$$\frac{cn}{2\pi u}|\vec{E}_{sp}^{\,macr}|^2 = \frac{\hbar\omega}{V} \tag{15}$$

On the left-hand side of Eq. (15) is an expression for the energy density in terms of the amplitude of the macroscopic electric field oscillations; the expression remains valid in the case of dispersive media, see §80 and Eq. (83.9) in [13]. On the right-hand side the energy density is expressed as the ratio of the energy of one photon to the box volume.

In the case of an induced transition, the amplitude of macroscopic electric field oscillations must be normalized to the energy flux density in the inducing radiation. If the inducing radiation intensity is denoted I and expressed in photons per unit time per unit area, then the normalization condition is

$$\frac{cn}{2\pi}\sum_{osc}|\vec{E}_{ind}^{\,macr}|^2 = \hbar\omega I \tag{16}$$

On the left-hand side of Eq. (16) there is an expression for the energy flux density in terms of a sum over all field oscillators of the squared amplitudes of the macroscopic electric field oscillations; the expression remains valid in the case of dispersive media, see §80 and Eq. (83.11) in [13]. On the right-hand side the energy flux density is expressed as the product of the energy of one photon and photon flux density.

This last paragraph is intended only for physicists. Note, that the expressions for the energy density in Eq. (15) and energy flux density in Eq. (16) differ from those in reference [13] in two ways. First, in Eqs. (15, 16) the refractive index has been substituted for the square root of the ratio of the dielectric permittivity to the magnetic permeability; this substitution is justified because at any frequency within the optical range the magnetic permeability equals unity. Second, in the denominator of Eqs. (15, 16) there is 2π instead of 8π in the corresponding Eqs. (83.9, 83.11) in [13]. This stems from the difference in the definitions of plane monochromatic waves: here a plane monochromatic wave is defined as a sum of two terms containing $e^{-i\omega t}$ and $e^{+i\omega t}$, same as in Ref. [16], while in [13] it is defined as one half of the sum. The terms containing $e^{-i\omega t}$ and $e^{+i\omega t}$ directly correspond to the operators of photon annihilation and creation [12], and this explains why we do not want them to be multiplied by 1/2.

Spontaneous Emission

The rate at which excited molecules emit photons varies with the intensity of the inducing electromagnetic radiation; however, when the intensity approaches zero, the emission rate approaches a nonzero limit. This limiting rate, expressed in photons per unit time per one excited molecule, is usually called the spontaneous emission rate and denoted by the capital gamma (Γ). Einstein called the same quantity coefficient A for spontaneous

emission [17]. In the field of fluorescence spectroscopy the same quantity is also known as the radiative decay rate or the reciprocal of the natural lifetime:

$$\Gamma = A_{Einstein} = k_r = \frac{1}{\tau_0} \tag{17}$$

Quantum-mechanical theory of transitions under the action of a periodic perturbation [11], which is also known as Fermi's golden rule, gives the following expression for Γ in the case of electric dipole coupling [14, 16]:

$$\Gamma = \frac{2\pi}{\hbar}\left\langle |\vec{E}_{sp}^{loc} \cdot \vec{\mu}_{01}|^2 \right\rangle_{osc} \rho(\omega) \tag{18}$$

Here $\langle \ldots \rangle_{osc}$ denotes averaging over all field oscillators with the frequencies equal to ω, ω equals the absolute value of the transition frequency ω_{01}, ω_{01} and $\vec{\mu}_{01}$ are defined in Eqs. (8,9), $\vec{E}_{sp}^{loc}$ is the amplitude of the local electric field oscillations where the fluorescent molecule is located, the dot denotes a scalar product of the two vectors, and $\rho(\omega)$ is defined in Eq. 12.

If the system is isotropic on both macroscopic and microscopic levels, then averaging over all field oscillators is a trivial task. In any system isotropic on the microscopic level

$$\vec{E}_{sp}^{loc} = f\vec{E}_{sp}^{macr} \tag{19}$$

where f is a scalar factor, the actual value of which depends on the cavity model; see later in this article. In any system isotropic on the macroscopic level the direction of the vector $\vec{E}_{sp}^{macr}$ is completely random, thus

$$\left\langle |\vec{E}_{sp}^{loc} \cdot \vec{\mu}_{01}|^2 \right\rangle_{osc} = \frac{1}{3} f^2 |\vec{E}_{sp}^{macr}|^2 |\vec{\mu}_{01}|^2 \tag{20}$$

$|\vec{E}_{sp}^{macr}|^2$can be expressed from Eq. (15) and substituted in Eq. (20):

$$\left\langle |\vec{E}_{sp}^{loc} \cdot \vec{\mu}_{01}|^2 \right\rangle_{osc} = \frac{2\pi\,\hbar u f^2 \omega}{3cnV} |\vec{\mu}_{01}|^2 \tag{21}$$

The latter expression and the expression for $\rho(\omega)$ from Eq. (13) can be substituted in Eq. (18); this gives

$$\Gamma = \frac{4f^2 n\omega^3}{3\hbar c^3} |\vec{\mu}_{01}|^2 \tag{22}$$

Note, that the box volume V that entered in the numerator in Eq. (13) and in the denominator in Eq. (21) has canceled out in the final expression for the spontaneous emission rate, exactly as it was promised earlier in this article. What is more important, the group velocity u that entered in the denominator in Eq. (13) and in the numerator in Eq. (21) has also canceled out. This result was explicitly brought up in Ref. [18], and it has a very important implication for fluorescence in dispersive media. High dispersion of the refractive index is expected for any medium in the spectral range near a strong absorption band (here the absorption band of the host medium and not of the fluorescent molecule is meant) [13]. CS_2, benzene, and other aromatic solvents are highly dispersive in the visible and, especially, in the near-UV spectral range. The density of field oscillators $\rho(\omega)$ can increase severalfold in a highly dispersive medium. Because the fundamental expression for the spontaneous emission rate contains $\rho(\omega)$, see Eq. (18), it is tempting to conclude that the spontaneous emission rate can be severalfold higher in a highly dispersive medium. The conclusion is false, because the group velocity u, which represents a quantitative measure of the refractive index dispersion, did not enter in the final expression for Γ, see Eq. (22). Thus the radiative rate in a medium with a high density of field oscillators is exactly the same as in a medium with a low density of field oscillators if both media have the same refractive index n. Out of all quantities in Eq. (22) only f and n depend on the characteristics of the host medium, and f is a function of n, see the discussion of cavity models.

Absorption and Stimulated Emission

Absorption and stimulated emission are in essence electronic transitions induced by electromagnetic radiation. When exposed to the radiation of an appropriate frequency, ground-state molecules make transitions to the excited state (absorption), and excited-state molecules make transitions to the ground state (stimulated emission). The rates of these processes in photons per unit time per 1 molecule will be denoted k_{ind}. Quantum-mechanical theory of transitions under the action of a periodic perturbation [11], which is also known as Fermi's golden rule, gives the following expression for k_{ind} in the case of electric dipole coupling:

$$k_{ind} = \frac{2\pi}{\hbar} \sum_{osc} |\vec{E}_{ind}^{loc} \cdot \vec{\mu}_{10}|^2 \, \delta(\hbar\omega - \hbar\omega_{10}) \tag{23}$$

Here $\sum_{osc}$ denotes summation over all field oscillators, $\vec{E}_{ind}^{loc}$ is the amplitude of the local electric field oscillations of the inducing wave at the location of the fluorescent molecule, $\vec{\mu}_{10}$ and ω_{10} are defined in Eqs. (8,9), the dot denotes a scalar product of two vectors, and $\delta(\ldots)$ is Dirac's delta-function.

If the local environment of the fluorescent molecule is isotropic, then

$$\vec{E}_{ind}^{loc} = f\,\vec{E}_{ind}^{macr} \tag{24}$$

where f is a scalar factor, the actual value of which depends on the cavity model, see later in this article. If, in addition to this, the inducing electromagnetic radiation is linearly polarized, and ϑ denotes the angle between the electric vector $\vec{E}_{ind}^{macr}$ and the transition moment $\vec{\mu}_{10}$, then

$$|\vec{E}_{ind}^{loc} \cdot \vec{\mu}_{10}|^2 = f^2\,|\vec{E}_{ind}^{macr}|^2\,|\vec{\mu}_{10}|^2\cos^2(\vartheta) \tag{25}$$

The expression on the right-hand side of Eq. (25) can be substituted for $|\vec{E}_{ind}^{loc} \cdot \vec{\mu}_{10}|^2$ in Eq. (23).

Then $\sum_{osc}|\vec{E}_{ind}^{macr}|^2$ can be expressed from Eq. (16) and substituted in the resulting equation. This yields

$$k_{ind} = \frac{4\pi^2\omega f^2}{cn}|\vec{\mu}_{10}|^2\,\delta(\hbar\omega - \hbar\omega_{10})\cos^2(\vartheta)\,I \tag{26}$$

Eq. (26) shows that the rates of induced transitions (k_{ind}) are directly proportional to the intensity of the inducing radiation (I). It is convenient to introduce the coefficient of proportionality

$$\sigma(\omega) = \frac{4\pi^2\omega f^2}{cn}\,|\vec{\mu}_{10}|^2\,\delta(\hbar\omega - \hbar\omega_{10})\cos^2(\vartheta) \tag{27}$$

$$k_{ind} = \sigma\,(\omega)\,I \tag{28}$$

The expression for $\sigma(\omega)$ in Eq. (27) contains Dirac's delta-function, which makes it inadequate for practical applications. The delta-function can be eliminated by integrating both sides of Eq. (27) over any frequency interval (ω_{min}, ω_{max}) containing the transition frequency ω_{10}. For reasons that will become evident in the next section, it is convenient to divide both sides of Eq. (28) by ω before integration, which yields

$$\int_{\omega_{min}}^{\omega_{max}} \frac{\sigma(\omega)}{\omega}d\omega = \frac{4\pi^2 f^2}{\hbar cn}\,|\vec{\mu}_{10}|^2\cos^2(\vartheta) \tag{29}$$

Effect of Nuclear Vibrations

Note, that throughout the previous two sections it was implied that a fluorescent molecule emitted and absorbed radiation of only one frequency, specifically, the electronic transition frequency ω_{10}. In the fixed-nuclei approximation the molecule is not expected to absorb or emit at any other frequency. It is the motion of the nuclei that broadens the absorption spectrum and the emission spectrum. The motion of the nuclei can be accounted for by the use of Franck-Condon factors, which represent the fractional contributions from transitions to different final states of nuclear motion. A perfect definition of Franck-Condon factors and description of their properties can be found in Herzberg's book [10], however, Herzberg called Franck-Condon factors the overlap integrals.

To account for nuclear vibrations, the expression for the probability of spontaneous emission from Eq. (22) needs to be averaged over all fluorescence emission frequencies ω using Franck-Condon factors as the weights:

$$\Gamma = \left\langle \frac{4f^2 n\omega^3}{3\hbar c^3}\,|\vec{\mu}_{01}|^2 \right\rangle_{fcf} \tag{30}$$

Here $\langle\ldots\rangle_{fcf}$ denotes Franck-Condon–weighted averaging. Frequency-invariant factors can be taken out of $\langle\ldots\rangle_{fcf}$. Strictly speaking, both the refractive index n and the local field correction factor f vary with frequency, but in those cases in which the difference between the values of n at the opposite ends of the emission spectrum does not exceed a few percent, the frequency variation of n and f (which is a function of n; see the description of cavity models) can be neglected. This yields

$$\Gamma = \frac{4f^2 n}{3\hbar c^3}|\vec{\mu}_{01}|^2\,\langle\omega^3\rangle_{fcf} \tag{31}$$

The value of $\langle\omega^3\rangle_{fcf}$ can be calculated from the shape of the emission spectrum. Because the emission at any frequency ω is proportional to the product of ω^3 and the corresponding Franck-Condon factor, the envelope of Franck-Condon factors for emission is equal to the emission spectrum multiplied by ω^{-3}. If $F_\omega(\omega)$ is the emission spectrum corrected to photons per unit frequency range, then $\omega^{-3}F_\omega(\omega)$ represents the envelope of Franck-Condon factors for emission. This yields the following expression for $\langle\omega^3\rangle_{fcf}$:

$$\langle\omega^3\rangle_{fcf} = \frac{\int\omega^3[\omega^{-3}F_\omega(\omega)]d\omega}{\int[\omega^{-3}F_\omega(\omega)]d\omega} = \frac{\int F_\omega(\omega)d\omega}{\int\omega^{-3}F_\omega(\omega)d\omega} \tag{32}$$

All integrals in Eq. (32) are definite and the integration is over the entire emission spectrum.

Franck-Condon–factor weighted averaging over all absorption frequencies (ω) must be performed on the expressions involving the probability of absorption. The final expression in this line is Eq. (29). Averaging of both sides of Eq. (29) over all ω is a trivial task, because neither side varies with ω. The left-hand side of Eq. (29) is a definite integral. The right-hand side of Eq. (29) does not contain ω explicitly, and the frequency variation of n

and f can be usually neglected. Thus the averaging leaves Eq. (29) practically unchanged:

$$\int_{\omega_{min}}^{\omega_{max}} \frac{\sigma(\omega)}{\omega} d\omega = \frac{4\pi^2 f^2}{\hbar c n} |\vec{\mu}_{10}|^2 \cos^2(\vartheta) \qquad (33)$$

The only difference between Eq. (29) and Eq. (33) is that in the former the interval (ω_{min}, ω_{max}) must contain the electronic transition frequency ω_{10}, and in the latter the interval (ω_{min}, ω_{max}) must contain the entire absorption band corresponding to the electronic transition 1←0.

EXPRESSIONS FOR PRACTICAL APPLICATION

Radiative Decay Rate

Circular frequency ω is rarely used in experimental work. Absorption and emission spectra are usually recorded as a function of wavelength λ or wavenumber $\bar{\nu}$. For this reason the expression for the radiative decay rate from Eq. (31) should be converted from ω to $\bar{\nu}$:

$$k_r \equiv \Gamma = \frac{64\pi^4}{3h} |\vec{\mu}_{01}|^2 \langle \bar{\nu}^3 \rangle_{fcf} f^2 n \qquad (34)$$

Here h is Planck's constant, $|\vec{\mu}_{01}|^2$ is defined in Eq. (8), $\langle \bar{\nu}^3 \rangle_{fcf}$ is the Franck-Condon–factor weighted average cube of the emission wavenumber, f is the local field correction factor (for details see the discussion of cavity models), and n is the refractive index of the host medium (solvent). Depending on whether the fluorescence emission spectrum is expressed as a function of wavelength or wavenumber, $\langle \bar{\nu}^3 \rangle_{fcf}$ should be calculated using Eq. (35) or Eq. (36):

$$\langle \bar{\nu}^3 \rangle_{fcf} = \frac{\int F_\lambda(\lambda) d\lambda}{\int \lambda^3 F_\lambda(\lambda) d\lambda} \qquad (35)$$

$$\langle \bar{\nu}^3 \rangle_{fcf} = \frac{\int F_\nu(\bar{\nu}) d\bar{\nu}}{\int \bar{\nu}^{-3} F_\nu(\bar{\nu}) d\bar{\nu}} \qquad (36)$$

Here F_λ is corrected to photons per unit wavelength range and F_ν is corrected to photons per unit wavenumber or unit frequency range; all the integrals are definite and the integration is carried out over the entire emission spectrum. Note, that $\langle \nu_f^{-3} \rangle_{Av}^{-1}$ in Strickler and Berg equation, Eq. (6), equals $c^3 \langle \bar{\nu} \rangle_{fcf}$.

Extinction Coefficient

The quantity σ was introduced earlier as the coefficient of proportionality between the rate (k_{ind}) of induced transitions and the intensity (I) of the inducing radiation [see Eq. (28)]. In the case of absorption, k_{ind} represents the number photons absorbed by 1 molecule per unit time and the excitation intensity I is measured in photons per unit time per unit area; therefore the coefficient of proportionality σ has the units of area per 1 molecule. The latter was the basis for the name "absorption cross section" that was given to σ during the time when the corpuscular theory of light was in favor. According to that theory, photons were tiny bullets, the molecule was a target, and σ was the area of the target. However, according to modern physics, a photon does not have a trajectory [12]; therefore it can neither hit nor miss a target, and the analogy between σ and target area falls apart. In light of this, the absorption cross section σ is simply a coefficient of proportionality between k_{ind} and I, and it is not related to the cross section of the molecule or any of its components.

For a dilute isotropic solution containing N absorbing solute molecules per unit volume in a transparent solvent, the absorption coefficient α equals the product of N and $\langle \sigma \rangle$, where $\langle \sigma \rangle$ denotes the mean absorption cross section (averaged over all possible orientations of the solute molecules with respect to the direction of polarization of the light wave):

$$\alpha = N \langle \sigma \rangle \qquad (37)$$

As the light wave propagates through the solution along the axis X, its intensity decreases according to Bouguer law

$$I = I_0 e^{-\alpha x} \qquad (38)$$

From Eqs. (37, 38) follows the relationship between the intensity of the incident light (I_0) and that of the light transmitted through the solution (I_T) for a cuvette with the path length L:

$$\ln (I_0/I_T) = \langle \sigma \rangle N L \qquad (39)$$

Now compare Eq. (39) with Eq. (40), which serves as the definition of the decadic molar extinction coefficient ε:

$$\log_{10} (I_0/I_T) = \langle \varepsilon \rangle C_{molar} L \qquad (40)$$

There are three differences between Eq. (39) and Eq. (40): (i) the logarithm is natural in the former and decadic in the latter, (ii) the concentration of the absorbing species is in molecules per unit volume (N) in the former and in moles per unit volume (C_{molar}) in the latter, and (iii) the role of the extinction coefficient is played by σ in the

former and by ε in the latter. If ε is called the decadic molar extinction coefficient, then σ may be called the natural molecular extinction coefficient. Thus the terms absorption cross section and natural molecular extinction coefficient are synonymous; both refer to σ.

From Eqs. (39, 40) follows a simple relationship between σ and ε:

$$\sigma = \frac{\ln(10)}{N_A}\varepsilon \tag{41}$$

Here N_A denotes Avogadro's number (the number of molecules per mole). Note that the decadic molar extinction coefficient ε is often expressed in $\mathrm{mol}^{-1}.\mathrm{dm}^3.\mathrm{cm}^{-1}$. Before ε can be substituted in Eq. (41), or in any other physical equation, it must be converted to consistent units. The presence of both dm and cm in one equation is intolerable in physics.

Both σ and ε vary with the wavelength λ of the exciting light; the functions that describe this variation will be denoted as $\sigma(\lambda)$ and $\varepsilon(\lambda)$. The functions $\sigma(\lambda)$ and $\varepsilon(\lambda)$ for a single molecule depend on the angle ϑ between the direction of its transition dipole moment $\vec{\mu}_{10}$ and the direction of polarization of the exciting light. From Eq. (33) it follows that

$$\int_{\lambda_{min}}^{\lambda_{max}} \frac{\sigma(\lambda)}{\lambda} d\lambda = \frac{8\pi^3}{hc} |\vec{\mu}_{10}|^2 \frac{f^2}{n} \cos^2(\vartheta) \tag{42}$$

Using the relationship between σ and ε in Eq. (41), a similar equation can be written for ε:

$$\frac{\ln(10)}{N_A} \int_{\lambda_{min}}^{\lambda_{max}} \frac{\epsilon(\lambda)}{\lambda} d\lambda = \frac{8\pi^3}{hc} |\vec{\mu}_{10}|^2 \frac{f^2}{n} \cos^2(\vartheta) \tag{43}$$

In Eqs. (42, 43) the integration wavelength range ($\lambda_{\min}$, $\lambda_{\max}$) must include the entire absorption band corresponding to the electronic transition $1 \leftarrow 0$ and no other absorption bands; h is Planck's constant, c is the speed of light in vacuum, $|\vec{\mu}_{10}|^2$ is defined in Eq. (8), f is the local field correction factor (for details see the next section), and n is the refractive index of the host medium.

In solution different solute molecules have different values of the angle ϑ, therefore their absorption cross sections and extinction coefficients are also different. The experimentally measured values $\langle\sigma\rangle$ and $\langle\varepsilon\rangle$ represent averages over all orientations of the solute molecules. For isotropic solutions $\langle\cos^2(\theta)\rangle = 1/3$, which yields

$$\int_{\lambda_{min}}^{\lambda_{max}} \frac{\langle\sigma(\lambda)\rangle}{\lambda} d\lambda = \frac{8\pi^3}{3hc} |\vec{\mu}_{10}|^2 \frac{f^2}{n} \tag{44}$$

$$\frac{\ln(10)}{N_A} \int_{\lambda_{min}}^{\lambda_{max}} \frac{\langle\varepsilon(\lambda)\rangle}{\lambda} d\lambda = \frac{8\pi^3}{3hc} |\vec{\mu}_{10}|^2 \frac{f^2}{n} \tag{45}$$

Note that Eqs. (44, 45) are valid only for isotropic solutions; they are not valid for molecules adsorbed to surfaces, solutions placed in strong electric fields (Stark effect), stretched polymer films (Polaroid), and crystals (including protein crystals).

Eqs. (42–45) make it clear that none of the quantities σ, ε, $\langle\sigma\rangle$, or $\langle\varepsilon\rangle$ represent an intrinsic property of a fluorescent molecule: all four quantities depend on the parameters f and n, which represent optical characteristics of the host medium. In addition to this, σ and ε depend on the angle ϑ, which changes whenever the molecule rotates or the direction of polarization of the exciting light is rotated. The quantities $\langle\sigma\rangle$ and $\langle\varepsilon\rangle$ represent ensemble averages rather than intrinsic properties of individual molecules.

The absorption cross section σ of a single molecule depends on its orientation as $\cos^2(\vartheta)$, and in isotropic solutions it covers the range from 0 to $3\langle\sigma\rangle$. Likewise, ε covers the range from 0 to $3\langle\varepsilon\rangle$. In some cases this must be taken into account. However, in most cases the difference in the extinction coefficient between individual absorbing solute molecules of the same type is not important. For example, if the duration of the exciting pulse is much longer than the rotational correlation time of the solute molecules, then the probability of excitation is approximately equal for all the molecules. In those cases in which the difference between σ and $\langle\sigma\rangle$ and between ε and $\langle\varepsilon\rangle$ does not have to be taken into account, the angle brackets are usually omitted for notation simplicity, and the symbol ε is used for the mean decadic molar extinction coefficient. This is the case for the most part of physical and chemical literature. In the following section no difference will be made between σ and $\langle\sigma\rangle$ and between ε and $\langle\varepsilon\rangle$; all equations there are equally applicable to the mean values and to the values for individual molecules.

CAVITY MODELS

The relationship between the macroscopic and local electric field depends on the geometry of the local environment. If the local environment is isotropic, then the relationship is

$$\vec{E}^{loc} = f\vec{E}^{macr} \tag{46}$$

where f is a scalar factor. This relationship was used in the derivation of the expressions for both the radiative decay rate and the extinction coefficients, and each of the

quantities k_r, σ and ε is directly proportional to f^2, see Eqs. (34, 42–45). These equations can be rewritten in a form that emphasizes the effects of the optical properties of the host medium:

$$k_r \equiv \Gamma = f^2 n \Gamma_0 \tag{47}$$

$$\sigma(\lambda) = \frac{f^2}{n}\,\sigma_0(\lambda) \tag{48}$$

$$\varepsilon(\lambda) = \frac{f^2}{n}\,\varepsilon_0(\lambda) \tag{49}$$

Here Γ_0, $\sigma_0(\lambda)$, and $\varepsilon_0(\lambda)$ are completely independent of the optical properties of the medium; expressions for these quantities in terms of fundamental parameters can be obtained by substituting $f = 1$ and $n = 1$ in Eqs. (34, 42–45). For example, here is the expression for Γ_0:

$$\Gamma_0 = \frac{64\pi^4}{3h} |\vec{\mu}_{01}|^2 \langle \bar{\nu}^3 \rangle_{fcf} \tag{50}$$

In the following four sections, four physical models of local environment will be considered; each model results in its own expression for f in terms of the macroscopic refractive index n.

Fluorescent Molecule Superimposed on Top of an Ideal Medium

An ideal medium is continuous on the microscopic level. If a fluorescent molecule is superimposed on top of the ideal medium (this implies that the molecule and the medium occupy the same volume), then the molecule interacts directly with $\vec{E}^{macr}$; therefore $f = 1$ and

$$k_r \equiv \Gamma = n\Gamma_0 \tag{51}$$

$$\sigma(\lambda) = n^{-1}\,\sigma_0(\lambda) \tag{52}$$

$$\varepsilon(\lambda) = n^{-1}\,\varepsilon_0(\lambda) \tag{53}$$

Although it is quite obvious that this model is not realistic, it has been used by Förster [19] and by many other authors.

Lorentz Virtual Cavity Model

By introducing a hypothetical (virtual) spherical cavity with the medium both outside and inside, Lorentz derived a relationship between the local and macroscopic field [20]. The relationship is equivalent to Eq. (46), where

$$f = \frac{n^2 + 2}{3} \tag{54}$$

Substituting this expression for f in Eqs (47–49) yields

$$k_r \equiv \Gamma = \left(\frac{n^2 + 2}{3}\right)^2 n\,\Gamma_0 \tag{55}$$

$$\sigma(\lambda) = \left(\frac{n^2 + 2}{3}\right)^2 n^{-1}\sigma_0(\lambda) \tag{56}$$

$$\varepsilon(\lambda) = \left(\frac{n^2 + 2}{3}\right)^2 n^{-1}\varepsilon_0(\lambda) \tag{57}$$

Although Eqs. (55–57) are based on the work of Lorentz, these equations were not invented by him, they were introduced by other authors who applied Lorentz local field theory to absorption [18,21–23] and to fluorescence emission [18,24–34]. Note that in Refs. [25–28,30–34] the virtual spherical cavity model is compared to the empty spherical cavity model (see the next section). The virtual spherical cavity model was also employed to calculate the local field correction to the rate of nonradiative resonance energy transfer [35]. Shibuya extended the virtual cavity model to the case of an ellipsoidal rather than spherical cavity shape [36,37].

Note that applying Lorentz local field correction to a molecule that absorbs or emits light results in a contradiction with an underlying assumption. In the derivation of the relationship between the local and macroscopic field, Lorentz made an explicit assumption that the molecule inside the cavity has the same polarizability as all other molecules of the medium [20]. Other authors made this assumption implicitly; for example, by writing Eq. (30) in Ref. [36] Shibuya implicitly assumed that the polarizability of the medium inside the ellipsoidal cavity is the same as if it had the refractive index of the outside medium. Unfortunately, this assumption is not valid if the molecule inside the cavity is not the same as the molecules of the host medium. This means that in the case in which absorption or emission is due to foreign molecules embedded in a host medium, the virtual cavity model does not apply.

Some authors argue that the virtual cavity model is applicable at least in the case in which there are no foreign molecules and absorption and emission are due to the molecules of the main medium [28]. This would be true if all the molecules were not only chemically identical but also in identical electronic states. However, absorption and emission of light involve electronic transitions, and an excited-state molecule does not have the same polarizability as the ground-state molecule. At a near-resonance frequency the polarizability of an excited-state molecule is approximately equal to $-\alpha$, where α denotes the

polarizability of the same molecule in the ground state. A molecule in transition between the ground state and the excited state has indefinite polarizability. From this one may conclude that the virtual cavity model is inapplicable regardless of whether the absorption and emission are due to foreign molecules or to the molecules of the main medium. This does not imply that Lorentz relationship between the local and macroscopic field is wrong; the relationship is valid for any isotropic homogeneous medium containing only ground-state molecules of one kind. Lorentz studied only media of this type in his work [20].

Empty Spherical Cavity Model

In the case of a fluorescent molecule in solution, the solvent is expelled from the volume occupied by the fluorescent molecule. This creates a cavity, in which the fluorescent molecule is located. It is necessary to relate the local field in the cavity to the macroscopic field outside the cavity. The optical-frequency polarizability of a fluorescent molecule in transition between the excited state and the ground state is indefinite, thus in the framework of classical field theory it is impossible to take into account the effect of the fluorescent molecule on the local field inside the cavity. An obvious alternative is to ignore the effect of the fluorescent molecule on the local field. This means that in deriving the relationship between the local field inside the cavity and the macroscopic field outside the cavity one must assume that the cavity is empty. Empty cavity models are described in this and the following section.

The empty spherical cavity model is also known as the real cavity model (in contrast to the virtual cavity model) and Glauber-Lewenstein model, by the names of the authors who suggested it first [15]. It is interesting that in an earlier paper [14] Yablonovitch, Gmitter, and Bhat wrote equations that could be made identical to those of the empty spherical cavity model by substituting $n_{int} = 1$, but the substitution was not made. The empty spherical cavity model results in the following expression for the factor f in Eq. (46),

$$f = \frac{3n^2}{2n^2 + 1} \tag{58}$$

and in the following expressions for k_r, σ and ε:

$$k_r \equiv \Gamma = \left(\frac{3n^2}{2n^2 + 1}\right)^2 n\,\Gamma_0 \tag{59}$$

$$\sigma(\lambda) = \left(\frac{3n^2}{2n^2 + 1}\right)^2 n^{-1}\sigma_0(\lambda) \tag{60}$$

$$\varepsilon(\lambda) = \left(\frac{3n^2}{2n^2 + 1}\right)^2 n^{-1}\varepsilon_0(\lambda) \tag{61}$$

Eqs. (58, 59) or their equivalents can be found in a large number of recent publications [15,25–28, 30–34,38–40]. Eqs. (60, 61) cannot be found in the literature, although they directly follow from Eq. (58). Apparently, the authors who used the empty spherical cavity model to calculate the spontaneous emission rate were not interested in the absorption cross section and the extinction coefficient. On the contrary, the interest in medium effects on the spontaneous emission rate is so high that hundreds of papers on this subjects have recently been published; only some of them are quoted here. Perhaps the most general study of spontaneous emission in condensed media was presented by Tkalya [39,40], who derived equations not only for electric dipole emission, but also for magnetic dipole emission, electric and magnetic quadrupole emissions, and electric and magnetic emissions of an arbitrary multipolarity. All equations in this article apply to electric dipole emission only; this was explicitly stated earlier in this article.

Empty Ellipsoidal Cavity Model

Lorentz developed his theory for atoms in a cubic crystal lattice. The choice of the spherical cavity shape is adequate for a cubic lattice. The spherical cavity shape is also adequate for an atom in an atomic gas, such as helium, because a helium atom has a spherical symmetry. Polyatomic fluorescent molecules do not have spherical symmetry in the fixed-nuclei approximation. If a polyatomic molecule is allowed to rotate freely, then its complete wavefunction (including both electronic and nuclear coordinates) may still have spherical symmetry [11], and in this case the choice of the spherical cavity shape is still adequate. However, if for a polyatomic fluorescent molecule in solution the orientation-dependent part of the energy of the solute–solvent interaction is comparable with or greater than kT, then the rotation of this molecule is not free and the choice of the spherical cavity shape is inadequate.

Not every cavity shape is consistent with the electric dipole approximation. If the shape is neither spherical nor ellipsoidal, then the electric field inside the cavity is not uniform [13], and this means that the effects of quadrupole and higher multipole moments are not expected to be much smaller than the effect of the dipole moment. Thus only spherical and ellipsoidal cavity shapes lead to simple analytical expressions for the radiative decay rate, absorption cross section, and extinction coefficient. The idea of using ellipsoidal instead of spherical cavity shape

in connection with molecules that absorb and emit light belongs to Shibuya [36,37]. Unfortunately, Shibuya's work is based on the virtual cavity model; Shibuya did not realize that applying that model to molecules that absorb or emit light results in a contradiction with an underlying assumption (see discussion of the Lorentz virtual cavity model). The ellipsoidal cavity shape can be also used in combination with the empty cavity model; this combination is described below.

An ellipsoid has three principal axes. The factor f in Eq. (46) has a different value for the electric fields parallel to each principal axis [13]. Generally speaking, unless the electric field is parallel to one of the principal axes, Eq. (46) is not valid. In applications related to electronic transition probabilities, only the component of the electric field parallel to the corresponding transition moment $\vec{\mu}_{ji}$ is of importance; therefore, if $\vec{\mu}_{ji}$ is parallel to any one of the principal axes, then a limited use of Eq. (46) is justifiable, and the value of the factor f in this case is given by the expression [13,16,41]

$$f = \frac{n^2}{(1 - L_\mu)\, n^2 + L_\mu} \tag{62}$$

Substituting this expression for f in Eqs. (47–49) yields

$$k_r \equiv \Gamma = \frac{n^5}{[(1 - L_\mu)\, n^2 + L_\mu]^2}\, \Gamma_0 \tag{63}$$

$$\sigma(\lambda) = \frac{n^3}{[(1 - L_\mu)\, n^2 + L_\mu]^2}\, \sigma_0(\lambda) \tag{64}$$

$$\varepsilon(\lambda) = \frac{n^3}{[(1 - L_\mu)\, n^2 + L_\mu]^2}\, \varepsilon_0(\lambda) \tag{65}$$

An expression equivalent to a combination of Eq. (63) with Eq. (50) can be found in Ref. [16].

For L_μ in Eqs. (62–65) one should substitute L_X, L_Y, or L_Z, depending on whether the transition moment $\vec{\mu}_{ji}$ is parallel to the axis X, Y, or Z. Parameters L_X, L_Y, L_Z can have any values between 0 and 1, subject to a constraint $L_X + L_Y + L_Z = 1$. The actual values of L_X, L_Y, L_Z depend on the length of the ellipsoid semiaxes a_X, a_Y, a_Z; the greatest L always corresponds to the shortest semiaxis, and the smallest L always corresponds to the longest semiaxis. Specific values of L_X, L_Y, L_Z can be obtained by numerical integration [16,41]:

$$L_x = \int_0^\infty \frac{a_X\, a_Y\, a_Z\, ds}{2\sqrt{(s + a_X^2)^3\, (s + a_Y^2)\, (s + a_Z^2)}} \tag{66}$$

Similar expressions for L_Y and L_Z can be obtained from Eq. (66) by cyclical rotation of all subscripts, $X \to Y \to Z \to X$.

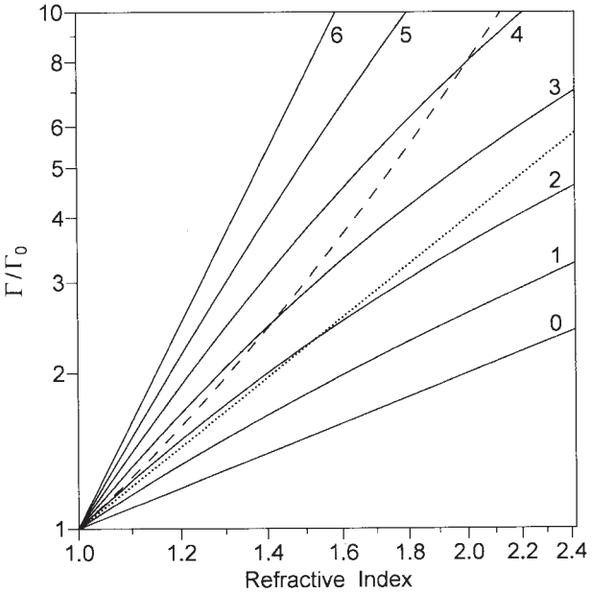

Fig. 1. Solvent refractive index variation of the radiative decay rate $k_r \equiv \Gamma$. The ratio Γ/Γ_0 is plotted on the logarithmic scale. Γ_0 is the limit of Γ at $n \to 1$. All curves are theoretical. Solid lines represent the empty ellipsoidal cavity model, Eq. (63); the value of the parameter L_μ for each curve equals one sixth of the number in the curve label. The curve labeled "2" also represents the empty spherical cavity model, Eq. (59). Broken line represents the virtual spherical cavity model, Eq. (55). Dotted line represents the law $\Gamma = \Gamma_0\, n^2$ that corresponds to no physical model.

For the special case of a sphere $L_X = L_Y = L_Z = 1/3$; substituting this value for L_μ in Eqs. (62–65) makes these equations equivalent to Eqs. (58–61). This shows that the empty spherical cavity model, also known as the real cavity model and Glauber-Lewenstein model, represents a special case of the empty ellipsoidal cavity model.

Graphical Review of Cavity Models

Variation of the radiative decay rate with the solvent refractive index for different cavity models is depicted in Fig. 1. Variation of the absorption cross section σ and the extinction coefficient ε for the same models is depicted in Fig. 2. The refractive index scale is logarithmic and covers the range from the refractive index of vacuum ($n = 1.00$) to that of diamond ($n = 2.42$ at 589 nm). The value of the radiative decay rate (Fig. 1) or the extinction coefficient (Fig. 2) is divided by the corresponding value in vacuum and is plotted on a logarithmic scale. The solid lines in each figure represent the empty ellipsoidal cavity model; different curves correspond to different values of L_μ. The value of L_μ for

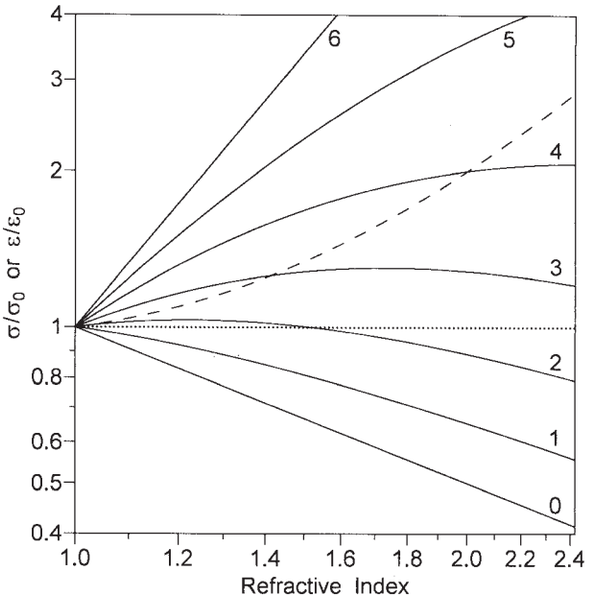

Fig. 2. Solvent refractive index variation of the absorption cross–section σ and extinction coefficient ε. The ratio $\sigma/\sigma_0 = \varepsilon/\varepsilon_0$ is plotted on the logarithmic scale. σ_0 and ε_0 are the limits of σ and ε at $n \to 1$. All curves are theoretical. Solid lines represent the empty ellipsoidal cavity model, Eqs. (64, 65); the value of L_μ for each curve equals one sixth of the number in the curve label. The curve labeled "2" also represents the empty spherical cavity model, Eqs. (60, 61). Broken line represents the virtual spherical cavity model, Eqs. (56, 57). Dotted line represents the law $\sigma = \sigma_0$, $\varepsilon = \varepsilon_0$ that corresponds to no physical model.

each curve equals one sixth of the number in the curve label. The curve labeled "2" corresponds to $L_\mu = 1/3$; therefore this curve also represents the empty spherical cavity model. The curve labeled "0" corresponds to $L_\mu = 0$; if this value is substituted in Eqs. (63–65), then these equations become equivalent to Eqs. (51–53); therefore the curve labeled "0" also represents the model of a fluorescent molecule superimposed on top of an ideal medium. The virtual spherical cavity model is represented by the broken lines in Figs. 1 and 2. Finally, the dotted lines in each figure represent the functions $\Gamma = \Gamma_0 n^2$, $\varepsilon = \varepsilon_0$. These functions do not follow from a physical theory, but they have been widely used [42–45].

The theoretical curves in Figs. 1 and 2 can be compared to experimental data, and based on the results of this comparison the model that provides the best fit can be selected. Note that on a logarithmic plot, where the vertical axis represents $\log(\Gamma/\Gamma_0)$, $\log(\sigma/\sigma_0)$, or $\log(\varepsilon/\varepsilon_0)$, the experimental data can be usually shifted up or down by redefining the value of the constant Γ_0, σ_0, or ε_0 (these constants are usually obtained by extrapolation of the experimental data to $n = 1$). Thus the value of the Y-intercept does not matter when experimental data are compared to a theoretical curve; the only thing that matters is the slope. The slope of a $\log(\Gamma/\Gamma_0)$ versus $\log(n)$ plot is the same as the slope of a $\log(\Gamma)$ versus $\log(n)$ plot. Likewise, the slopes of $\log(\sigma/\sigma_0)$ versus $\log(n)$ and $\log(\varepsilon/\varepsilon_0)$ versus $\log(n)$ plots are the same as the slopes of $\log(\sigma)$ versus $\log(n)$ and $\log(\varepsilon)$ versus $\log(n)$ plots. The slopes of the theoretical curves corresponding to the four physical models described above can be calculated using the following expressions, in which $+1$ should be substituted for ± 1 if $Y = \Gamma$ and -1 should be substituted for ± 1 if $Y = \sigma$ or $Y = \varepsilon$:

$$\frac{\partial \log(Y)}{\partial \log(n)} = \pm 1 \tag{67}$$

$$\frac{\partial \log(Y)}{\partial \log(n)} = \pm 1 + \frac{4n^2}{n^2 + 2} \tag{68}$$

$$\frac{\partial \log(Y)}{\partial \log(n)} = \pm 1 + \frac{4}{2n^2 + 1} \tag{69}$$

$$\frac{\partial \log(Y)}{\partial \log(n)} = \pm 1 + \frac{4L_\mu}{(1 - L_\mu)\, n^2 + L_\mu} \tag{70}$$

Eq. (67) corresponds to the model of a fluorescent molecule superimposed on top of an ideal medium (see discussion of fluorescent molecule imposition on an ideal medium). For this model the slope is constant and equals $+1$ in the case of the $\log(\Gamma)$ versus $\log(n)$ plot and -1 in the case of the $\log(\varepsilon)$ versus $\log(n)$ plot.

Eq. (68) corresponds to the virtual spherical cavity model. For this model the slope is not constant, and it increases with the refractive index. For a refractive index close to that of vacuum ($n = 1$), hexane ($n = 1.375$ at 589 nm), and CS_2 ($n = 1.632$ at 589 nm) the corresponding values of the slope are $+2.333$, $+2.944$, and $+3.285$ in the case of the $\log(\Gamma)$ versus $\log(n)$ plot and $+0.333$, $+0.944$, and $+1.285$ in the case of the $\log(\varepsilon)$ versus $\log(n)$ plot.

Eq. (69) corresponds to the empty spherical cavity model. For this model the slope is not constant, and it decreases with the refractive index. For a refractive index close to that of vacuum ($n = 1$), hexane ($n = 1.375$ at 589 nm), and CS_2 ($n = 1.632$ at 589 nm) the corresponding values of the slope are $+2.333$, $+1.837$, and $+1.632$ in the case of the $\log(\Gamma)$ versus $\log(n)$ plot and $+0.333$, -0.163 and -0.368 in the case of the $\log(\varepsilon)$ versus $\log(n)$ plot.

Eq. (70) corresponds to the empty ellipsoidal cavity model. For this model the slope depends on the value of the ellipticity parameter L_μ. For $L_\mu = 1/3$ the slope is the same as in the case of the empty spherical cavity model. For $L_\mu = 0$ and $L_\mu = 1$ the corresponding values of the slope are $+1$ and $+5$ in the case of the log (Γ) versus log(n) plot and -1 and $+3$ in the case of the log(ε) versus log(n) plot. Any slope between $+1$ and $+5$ for the log(Γ) versus log (n) plot can be achieved by selecting the appropriate value of L_μ. Likewise, any slope between -1 and $+3$ for the log(ε) versus log(n) plot can be achieved by selecting the appropriate value of L_μ.

EXPERIMENTAL EVIDENCE

There are very few experimental studies aimed specifically at discriminating between different cavity models [25,27,33]. In two of them the results confirmed the empty spherical cavity model [25,27]; these results are shown in the following section. In the third study the radiative decay rate was found to depend not solely on the refractive index, but also on some other property of the solvent [33]; possible explanations of this result are discussed later. Valuable experimental data regarding the solvent refractive index effect on the radiative decay rate can be also found in earlier publications [42,44,46], the authors of which were unaware of the physical theory of this effect. It will be shown that these data are in agreement with either the empty spherical cavity model or the empty ellipsoidal cavity model.

There are also a number of experimental studies of the solvent refractive index effect on the radiative decay rate, where the fluorescent molecule was inserted in a microscopic object, such as a lipid membrane [47–51], a reverse micelle [52–54], or a protein globule [16], and the microscopic object was immersed in the solvent of variable refractive index. The theoretical models describing the refractive index variation of the radiative decay rates in these systems are not identical to the models for a fluorescent molecule immersed directly in the solvent; therefore the results of experimental studies [16,47–54] cannot be used to discriminate among various cavity models.

Chelated Eu^{3+} in Non–Hydrogen-Bonding Solvents

In Ref. [25] the lifetime of the excited $^5D_0$ state of a chelated Eu^{3+} ion in Eu^{3+}–hfa–topo complex was measured in a series of apolar hydrocarbons and fluorocarbons. The radiative lifetime τ_0 (also known as the natural lifetime) was calculated from the values of the measured lifetime τ and the quantum yield η. The quantum yield was close to unity (e.g., in toluene $\eta = 0.95 \pm 0.05$); therefore the values of τ_0 and τ differed only slightly. In Fig. 3 the radiative lifetime is plotted versus the solvent refractive index. Note that although the vertical axis is labeled τ, it actually represents the radiative lifetime τ_0. The experimental data are shown by circles with error bars, and the lines represent the best fits to the experimental data by three different models. It is not difficult to see that the empty spherical cavity model (solid line) gives the best fit to the experimental data.

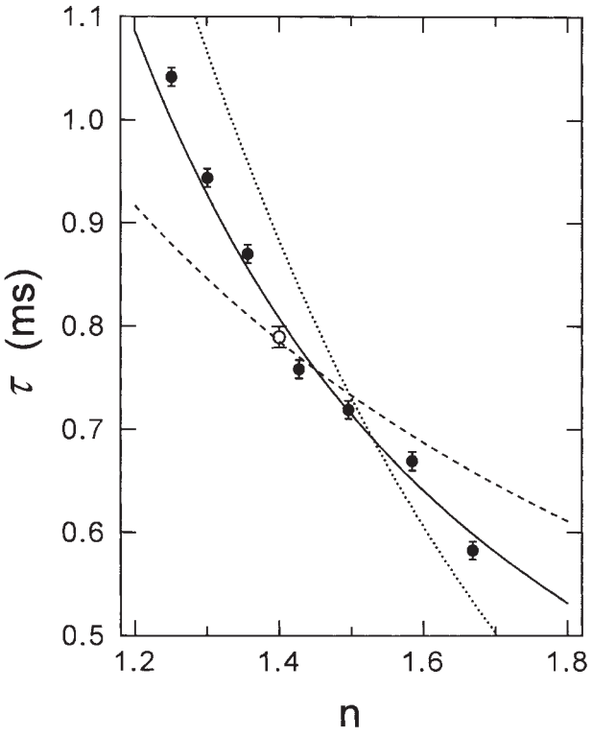

Fig. 3. Radiative lifetime of Eu^{3+}–hfa–topo dissolved in apolar hydrocarbons and fluorocarbons, as a function of the solvent refractive index. Reproduced from Ref. [25] with permission from the American Physical Society and from Dr. G. L. J. A. Rikken. Experimental data are shown by circles with error bars. Broken line represents the model of a fluorescent molecule superimposed on top of an ideal medium, Eq. (51). Dotted line represents the virtual spherical cavity model, Eq. (55). Solid line represents the empty spherical cavity model, Eq. (59).

In Ref. [27] the lifetime of the excited $^5D_0$ state of a chelated Eu^{3+} ion in $Eu(fod)_3$ complex was measured in supercritical CO_2. By changing pressure, the refractive index of a liquid heated just slightly above the critical temperature could be continuously varied over a wide range, starting from low values typical for gases and

ending with high values typical for common (nonsupercritical) liquids. Thus a supercritical liquid was a perfect solvent for a study of the refractive index effect. In addition to this, the nonradiative decay rate for the $^5D_0$ state of Eu(fod)$_3$ complex in liquid CO_2 is much smaller than the radiative decay rate; therefore the radiative lifetime τ_0 was assumed to be equal to the measured lifetime τ [27]. In Fig. 4 the ratio of the radiative lifetime in supercritical CO_2 to that in vacuum is plotted versus the solvent refractive index (the value of τ_R^{vac} was a result of extrapolation rather than direct measurement). Experimental data are shown by circles, squares, and triangles. The lines represent the best fits to the experimental data by three different models. The experimental data unambiguously confirm the empty spherical cavity model (solid line).

Chelated Eu^{3+} in Hydrogen-Bonding Solvents

In Ref. [33] the lifetime of Eu(fod)$_3$ complex was measured in a homologic series of simple alcohols. The results were found to be inconsistent with both virtual spherical cavity model and empty spherical cavity model. All theoretical models predict a monotonic increase of the radiative decay rate with the refractive index (Fig. 1), whereas the experimental data did not comply with this prediction. Furthermore, the data obtained with deuterated alcohols CH_3 $(CH_2)_mOD$ did not fall on the same line as the data obtained with common (protonated) alcohols $CH_3(CH_2)_mOH$. This result can be explained by the effect of hydrogen bonding. Note that if the fluorescent solute forms hydrogen bonds with the solvent, then it cannot rotate freely. For a molecule that neither has spherical symmetry nor can rotate freely, the choice of the spherical cavity shape is inappropriate. If we assume for instance that the cavity is ellipsoidal, then the radiative decay rate will depend not only on the refractive index of the solvent, but also on the ellipticity parameter L_μ. This parameter can have different values depending on the specific solvent; therefore it is not surprising that the experimental points in Ref. [33] did not fall on a single line. In the case of non–hydrogen bonding solvents, such as hydrocarbons and fluorocarbons [25] or CO_2 [27], the cavity was spherical and the ellipticity parameter L_μ had a constant value of one third, which explains why the experimental points there fell on one line. The explanation represented here is somewhat different than the one proposed by the authors of Ref. [33]. The conclusion of the authors was that the deviations from the empty spherical cavity model were "due to the subtle changes in the symmetry of the europium complex when dissolving it in different alcohols." Indeed, this is a possible explanation; however, it is equally possible that the spherical symmetry of the cavity and not the symmetry of the solute was destroyed in hydrogen-bonding solvents.

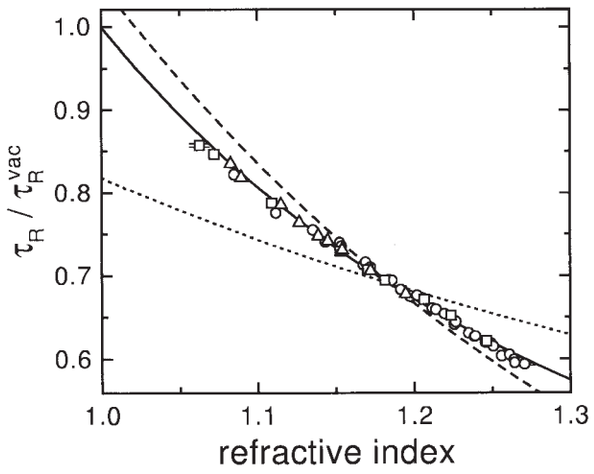

Fig. 4. The ratio of the radiative lifetime of Eu(fod)$_3$ dissolved in supercritical CO_2 to that in vacuum, as a function of the solvent refractive index (the value of τ_R^{vac} was a result of extrapolation rather than direct measurement). Reproduced from Ref. [27] with permission from the American Physical Society and from professor A. Lagendijk. Experimental data obtained in different series of measurements are shown by circles, squares, and triangles. Dotted line represents the model of a fluorescent molecule superimposed on top of an ideal medium, Eq. (51). Broken line represents the virtual spherical cavity model, Eq. (55). Solid line represents the empty spherical cavity model, Eq. (59).

9-Cyanoanthracene in Methylcyclohexane

In Ref. [42] the excited-state lifetimes of five anthracene derivatives were measured in methylcyclohexane. The refractive index of the solvent was varied from 1.4206 to 1.5473 by applying hydrostatic pressure between 0.1 MPa and 700 MPa. It is extremely difficult to measure the quantum yield of a solution in a high-pressure optical vessel. The authors of Ref. [42] selected the compounds with high quantum yields in methylcyclohexane and assumed that the quantum yields were close to unity. The assumption was verified by cooling solutions of the anthracene derivatives to 77 K. Based on this assumption, the radiative decay rate Γ can be calculated as $1/\tau$, where τ was the measured lifetime. The original data are available in the numerical format in Table I of Ref. [42]. The authors of Ref. [42] did not fit their data by a model function based on a physical theory; the fitting was done specifically for this article, and the best

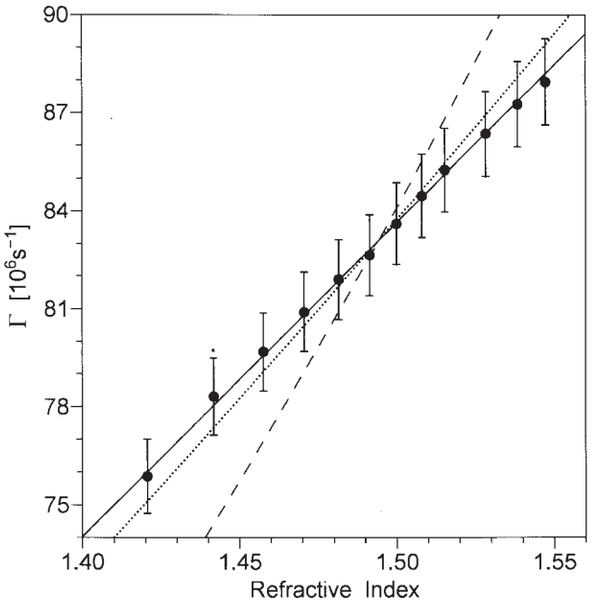

Fig. 5. The radiative decay rate of 9-cyanoanthracene dissolved in methylcyclohexane at hydrostatic pressures from 0.1 to 700 MPa, as a function of the solvent refractive index. Circles represent experimental data from Table I of Ref. [42]. Error bars correspond to ±1.5% errors, as specified in the footnote to Table I of Ref. [42]. *Broken line*: the best fit with the virtual spherical cavity model, Eq. (55). *Solid line*: the best fit with the empty spherical cavity model, Eq. (59). *Dotted line*: the best fit by the empirical function $\Gamma = \Gamma_0 n^2$, which corresponds to no physical model, but was suggested in Ref. [42].

fits are shown in Fig. 5. The data in Fig. 5 represent the radiative decay rate of 9-cyanoanthracene, which was selected out of the five anthracene derivatives because it appears to have the highest quantum yield. The empty spherical cavity model (solid line) results in a better fit, not only compared to the virtual spherical cavity model (broken line) but also compared to the empirical function $\Gamma = \Gamma_0 n^2$ (dotted line).

The difference between the solid line and the dotted line in Fig. 5 is quite small, and both lines fit the experimental data within the specified errors. One may want to increase the range of the refractive index variation so that the model curves would diverge more. Because the lifetime of 9-cyanoanthracene was also measured in a jet-cooled gas at low pressure [46], where $n = 1$; this result can be added to the experimental points in Fig. 5. In Fig. 6 the data from Fig. 5 are combined with the gas-phase result from Ref. [46]. The gas-phase result (square) is consistent with both the empty spherical cavity model (the solid line) and the empirical function $\Gamma = \Gamma_0 n^2$ (the dotted line), but it is clearly inconsistent with the virtual spherical cavity model (the broken line). To experimentally disprove the empirical function $\Gamma = \Gamma_0 n^2$, one would have to use solvents with the refractive index values over 1.8, because only for $n > 1.8$ this empirical function $\Gamma = \Gamma_0 n^2$ differs considerably from the model function corresponding to the empty spherical cavity model, see the dotted line and the solid line labeled "2" in Fig. 1.

Trans-Stilbene in n-Alkanes

In Ref. [44] the radiative decay rate of trans-stilbene in n-hexane and n-tetradecane was recorded as a function of the solvent refractive index. The refractive index of each solvent was varied by changing the temperature. The data were found to satisfy the empirical equation

$$\Gamma = \Gamma_0 n^x \tag{71}$$

where $x = 1.65 \pm 0.08$ and $\Gamma_0 = 3.75 \times 10^8 \text{s}^{-1}$ [44]. From Eq. (71) it follows that on a log(Γ) versus log(n) plot the data points fall on a straight line with the slope of 1.65 ± 0.08. It is interesting to compare this with the slopes of log(Γ) versus log(n) plots for the known cavity models. The curves shown in Fig. 1 make it apparent that for most models the slope changes with the refractive index. We are interested in comparing the slopes in the refractive index range between $n = 1.350$ (the refractive index of n–hexane at 70°C) and $n = 1.430$ (the refractive index of n–tetradecane at 18°C), because for this range the

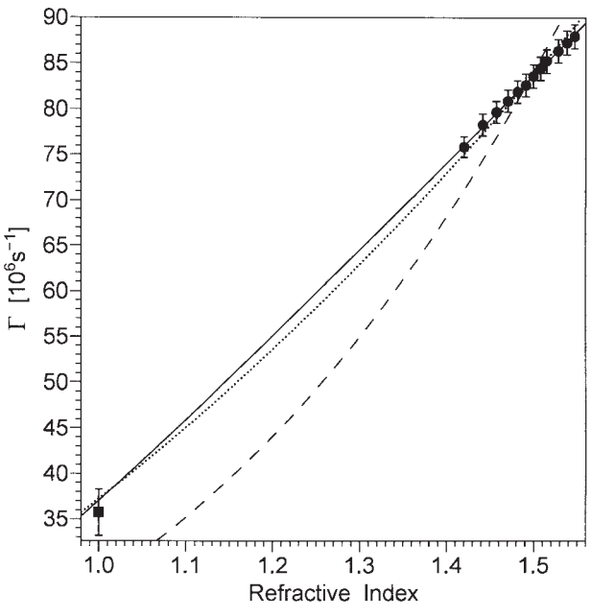

Fig. 6. The radiative decay rate of 9-cyanoanthracene as a function of the solvent refractive index. *Square*: the radiative decay rate of 9-cyanoanthracene in a jet-cooled gas at low pressure [46]. *Circles, broken, solid and dotted line*: see the legend of Fig. 5.

experimental data are available. The midpoint of this range corresponds to $n = 1.390$. Substituting this n value in Eqs. (67–69) yields the following slopes: 1.00 for the model of a fluorescent molecule superimposed on top of an ideal medium, 2.97 for the virtual spherical cavity model, and 1.82 for the empty spherical cavity model. The values of 1.00 and 2.97 are too far from the experimental value of 1.65 ± 0.08; this rules out the first two models. The slope for the empty spherical cavity model is much closer to the experimental value, but it is still greater than the upper limit of the confidence interval. In the case of an empty ellipsoidal cavity model the slope depends on the value of L_μ, and by choosing the appropriate value of L_μ one can match any slope between 1.00 and 5.00 in a narrow refractive index range. From Eq. (70) it follows that for $n = 1.390$ the slope of 1.65 is achieved with $L_\mu = 0.272$, and the slope range of 1.65 ± 0.08 corresponds to the L_μ range of 0.272 ± 0.029. All values in this L_μ range are lower than one third, which proves that the transition moment $\vec{\mu}_{01}$ is parallel to the longest axis of the ellipsoidal cavity. It is well known that in trans-stilbene the direction of the transition moment $\vec{\mu}_{01}$ coincides with the longest dimension of the molecule. From this we conclude that in the case of trans-stilbene in n-alkanes the longest axis of the ellipsoidal cavity has the same direction as the longest dimension of the solute molecule. This finding is consistent with the notion that the shape of the cavity must resemble the shape of the molecule.

DISTANCE CUTOFF FOR MEDIUM EFFECTS

In real life a fluorescent molecule is never placed in a homogeneous solvent of infinite dimensions, there is always a cuvette wall or another object at a finite distance from the molecule. If the distance to the foreign object is long enough, then the object has no effect on the spontaneous emission rate and the excitation rate. The cutoff distance at which the effects of all foreign objects vanish is estimated in this section. An easy way to obtain the estimate of the cutoff distance is based on a model system suggested by Drexhage [55]. Consider a spherical mirror made of a material with 100% reflectivity. The mirror has the shape of one half of a full sphere, as if the sphere was cut by a plane passing through its center, and one half was removed. A fluorescent molecule is placed at the center of the sphere. If the molecule had an infinitely narrow emission spectrum, then the radiative decay rate would be given by the equation

$$\Gamma = 2\sin^2(2\pi nR/\lambda)\,\Gamma_{WM} \tag{72}$$

Here Γ is the spontaneous emission rate of the fluorescent molecule at the center of the sphere, Γ_{WM} is the spontaneous emission rate of the same molecule in the same medium, but without the mirror, n is the refractive index of the medium, R is the radius of the sphere, and λ is the emission wavelength (measured in vacuum). If $2nR = m\lambda$, where m is an integer, then the radiative rate equals zero. If $2nR = (m + \frac{1}{2})\lambda$, then the radiative rate equals $2\Gamma_{WM}$. As the radius R increases, the radiative rate keeps oscillating between 0 and $2\Gamma_{WM}$, and there is no cutoff distance for this oscillation if the fluorescent molecule emits only one wavelength. Now consider emission at two different wavelengths, λ_1 and λ_2. If the condition

$$2nR/\lambda_1 - 2nR/\lambda_2 = \tfrac{1}{2} \tag{73}$$

is satisfied, then the emission at λ_1 reaches a peak value when the emission at λ_2 reaches zero and vice versa. It is convenient to convert Eq. (73) from wavelengths to wavenumbers:

$$2nR(\bar{\nu}_1 - \bar{\nu}_2) = \tfrac{1}{2} \tag{74}$$

If on the wavenumber scale the emission spectrum has a width $\Delta\bar{\nu}$ that satisfies the condition

$$2nR\,\Delta\bar{\nu} = 1 \tag{75}$$

then for any $\bar{\nu}_1$ within the emission spectrum one can always find a $\bar{\nu}_2$ within the emission spectrum so that for the pair the condition in Eq. (74) is satisfied. Eq. (75) can be resolved with respect to R, which will then give the cutoff distance for the emission spectrum of the width $\Delta\bar{\nu}$. Because this is a rough estimate, and the value of n is close to unity, omitting n from the expression for R_C is not going to make a big difference:

$$R_c = 1/(2\Delta\bar{\nu}) \tag{76}$$

Eq. (76) gives the cutoff distance for medium effects on both the spontaneous emission rate and the excitation rate; however, in the case of the emission rate one should substitute for $\Delta\bar{\nu}$ the width of the emission spectrum, whereas in the case of the excitation rate one should use the smaller of the absorption spectrum width and the exciting radiation bandwidth. For a laser source of visible light the radiation bandwidth may be so narrow, that R_C may exceed the distance between the cornea and the retina in the human eye. In this case the rate of excitation of individual rhodopsin molecules in the retina is affected by the interfaces between different media in the human eye, and a characteristic speckle pattern becomes visible.

SUMMARY

Based on previously published theoretical and experimental work of many authors it is fair to conclude that the empty spherical cavity model and the empty ellipsoidal cavity model give the most accurate description of the solvent refractive index effects on the radiative decay rates and extinction coefficients of fluorescent solutes. Generally speaking, the shape of the cavity from which a fluorescent molecule expels all solvent molecules depends not only on the shape of the fluorescent molecule but also on the physical nature of the solvent–solute interactions. If the potential energy of the solute–solvent interactions is independent of the solute orientation, the cavity shape is spherical. If the solute–solvent interactions involve hydrogen bonding or another type of bonding with solute-orientation–dependent bond energy, then the cavity shape may not be spherical. In this case the empty ellipsoidal cavity model is a better choice. The ellipsoidal model includes the spherical model as a special case. The ellipticity parameter L_μ can assume values between 0 and 1 depending on the cavity shape and the orientation of the electronic transition dipole moment responsible for absorption and emission. For a spherical cavity $L_\mu = \frac{1}{3}$. If the cavity is not spherical and the transition moment is parallel to its longest dimension, then $L_\mu < \frac{1}{3}$. If the transition moment is parallel to the shortest dimension of the cavity, then $L_\mu > \frac{1}{3}$. The radiative decay rate and the molar extinction coefficient vary with the solvent refractive index according to Eqs. (77, 78):

$$k_r \equiv \Gamma = \frac{n^5}{[(1 - L_\mu)\, n^2 + L_\mu]^2}\, \Gamma_0 \qquad (77)$$

$$\varepsilon(\lambda) = \frac{n^3}{[(1 - L_\mu) n^2 + L_\mu]^2}\, \varepsilon_0(\lambda) \qquad (78)$$

If the shapes of the absorption and emission spectra change between different solvents, it is also necessary to take into account that Γ_0 in Eq. (77) is directly proportional to $\langle \bar{\nu}^3 \rangle_{fcf}$, see Eqs. (50, 35, 36), and instead of Eq. (78), one should use

$$\int_{\lambda_{min}}^{\lambda_{max}} \frac{\varepsilon(\lambda)}{\lambda}\, d\lambda = \frac{An^3}{[(1 - L_\mu)\, n^2 + L_\mu]^2} \qquad (79)$$

where A is a constant factor and the wavelength interval (λ_{min}, λ_{max}) must completely include the absorption band corresponding to the electronic transition $1 \leftarrow 0$ and no other absorption bands. It is also necessary to take into account that the value of L_μ may differ from one solvent to another, especially in the case in which at least one of the solvents is hydrogen bonding.

ACKNOWLEDGMENTS

The author thanks his teachers, Professors M. D. Galanin, E. A. Sviridenkov, and V. M. Agranovich, who taught the author almost everything he knows about fluorescence. The author also thanks Professor L. Brand for valuable critical comments and Professor D. M. Fambrough for support. The work was supported by the National Institutes of Health grant NS23241.

REFERENCES

1. J. R. Lakowicz (1999) *Principles of Fluorescence Spectroscopy*, 2nd ed, Kluwer Academic/Plenum Press, New York.
2. Y. Ooshika (1954) Absorption spectra of dyes in solution. *J. Phys. Soc. Japan* **9**(4), 594–602.
3. N. Mataga, Y. Kaifu, and M. Koizumi (1956) Solvent effects upon fluorescence spectra and the dipolemoments of excited molecules. *Bull. Chem. Soc. Japan* **29**(4), 465–470.
4. E. McRae (1957) Theory of solvent effects on molecular electronic spectra: Frequency shifts. *J. Phys. Chem.* **61**(5), 562–572.
5. Von E. Lippert (1957) Spektroskopische bestimmung des dipolmomentes aromatischer verbindungen im ersten angeregten singulettzustand. Z. *Elektrochem.* **61**(8), 962–975.
6. N. G. Bakhshiev (1961) Universal molecular interactions and their effect on the position of the electronic spectra of molecules in two-component solutions 1: Theory (liquid solutions). *Optics Spectrosc.* **10**(6), 717–726.
7. F. Perrin (1926) Polarisation de la lumiere de fluorescence: Vie moyenne des molecules dans l'etat excite. *J. Phys. Radium* Serie 6, **7** (12), 390–401.
8. S. J. Strickler and R. A. Berg (1962) Relationship between absorption intensity and fluorescence lifetime of molecules. *J. Chem. Phys.* **37**(4), 814–822.
9. L. D. Landau and E. M. Lifshitz (1975) *The classical theory of fields*, 4th ed, Pergamon Press, New York.
10. G. Herzberg (1950) *Molecular Spectra and Molecular Structure: I. Spectra of Diatomic Molecules*, 2nd ed, D. Van Nostrand Co., New York.
11. L. D. Landau and E. M. Lifshitz (1977) *Quantum Mechanics: Non-Relativistic Theory*, 2nd ed, Pergamon Press, New York.
12. V. B. Berestetskii, E. M. Lifshitz, and L. P. Pitaevskii. (1982) *Quantum Electrodynamics*. 2nd ed. Pergamon Press, New York.
13. L. D. Landau and E. M. Lifshitz (1984) *Electrodynamics of Continuous Media*, 2nd ed, Pergamon Press, New York.
14. E. Yablonovitch, T. J. Gmitter, and R. Bhat (1988) Inhibited and enhanced spontaneous emission from optically thin AlGaAs/GaAs double heterostructures. *Phys. Rev. Lett.* **61**(22), 2546–2549.
15. R. J. Glauber and M. Lewenstein (1991) Quantum optics of dielectric media. *Phys. Rev. A* **43**(1), 467–491.
16. D. Toptygin, R. S. Savtchenko, N. D. Meadow, S. Roseman, and L. Brand (2002) Effect of the solvent refractive index on the excited-state lifetime of a single tryptophan residue in a protein. *J. Phys. Chem. B* **106**, 3724–3734.
17. A. Einstein (1917) Zur quantentheorie der strahlung. *Physik. Z.* **18**, 121–128.

18. G. Juzeliunas (1995) Molecule–radiation and molecule–molecule processes in condensed media: A microscopic QED theory. *Chem. Phys.* **198**(1–2), 145–158.
19. T. Förster (1951) *Fluoreszenz organischer Verbindungen*, Vandenhoeck & Ruprecht, Göttingen.
20. H. A. Lorentz (1909) *The Theory of Electrons and Its Applications to the Phenomena of Light and Radiant Heat.* Leipzig, Teubner.
21. N. Q. Chako (1934) Absorption of light in organic compounds. *J. Chem. Phys.* **2**, 644–653.
22. G. Kortüm (1936). Das optische verhalten gelöster ionen und seine bedeutung für die struktur elektrolytischer lösungen. *Z. Physik. Chem. (B)* **33**(4), 243–264.
23. W. Liptay (1966). Die lösungsmittelabhängigkeit der intensität von elektronenbanden. I. Theorie. *Z. Naturforschg. A* **21A**(10), 1605–1618.
24. S. M. Barnett, B. Huttner, and R. Loudon (1992) Spontaneous emission in absorbing dielectric media. *Phys. Rev. Lett.* **68**(25), 3698–3701.
25. G. L. J. A. Rikken and Y. A. R. R. Kessener (1995) Local field effects and electric and magnetic dipole transitions in dielectrics. *Phys. Rev. Lett.* **74**(6), 880–883.
26. S. M. Barnett, B. Huttner, R. Loudon, and R. Matloob (1996) Decay of excited atoms in absorbing dielectrics. *J. Phys. B: At. Mol. Opt. Phys.* **29**, 3763–3781.
27. F. J. P. Schuurmans, D. T. N. de Lang, G. H. Wegdam, R. Sprik, and A. Lagendijk (1998) Local-field effects on spontaneous emission in a dense supercritical gas. *Phys. Rev. Lett.* **80**(23), 5077–5080.
28. P. de Vries and A. Lagendijk (1998) Resonant scattering and spontaneous smission in dielectrics: Microscopic derivation of local-field effects. *Phys. Rev. Lett.* **81**(7), 1381–1384.
29. S. Scheel, L. Knöll, D.-G. Welsch, and S. M. Barnett (1999) Quantum local-field corrections and spontaneous decay. *Phys. Rev. A.* **60**(2), 1590–1597.
30. M. Fleischhauer (1999) Spontaneous emission and level shifts in absorbing disordered dielectrics and dense atomic gases: A Green's-function approach. *Phys. Rev. A* **60**(3), 2534–2539.
31. S. Scheel, L. Knöll, and D.-G. Welsch (1999) Spontaneous decay of an excited atom in an absorbing dielectric. *Phys. Rev. A.* **60**(5), 4094–4104.
32. F. J. P. Schuurmans, P. de Vries, and A. Lagendijk (2000) Local-field effects on spontaneous emission of impurity atoms in homogeneous dielectrics. *Phys. Lett. A* **264**(1), 472–477.
33. F. J. P. Schuurmans and A. Lagendijk (2000) Luminescence of $Eu(fod)_3$ in a homologic series of simple alcohols. *J. Chem. Phys.* **113**(8), 3310–3314.
34. M. S. Tomas (2001) Local-field corrections to the decay rate of excited molecules in absorbing cavities: The Onsager model. *Phys. Rev. A* **63**(5), 053811-1–053811-11.
35. V. M. Agranovich and M. D. Galanin (1982) *Electronic Excitation Energy Transfer in Condensed Matter*, North-Holland, Amsterdam.
36. T. Shibuya (1983) A dielectric model for the solvent effect on the intensity of light-absorption. *J. Chem. Phys.* **78**(8), 5175–5182.
37. T. Shibuya (1983) The refractive-index correction to the radiative rate constant. *Chem. Phys. Lett.* **103**(1), 46–48.
38. C. Q. Cao, W. Long, and H. Cao (1997) The local field correction factor for spontaneous emission. *Phys. Lett. A* **232**, 15–24.
39. E. V. Tkalya (2001) Spontaneous multipole radiation in a condensed medium. *J. Exper. Theoret. Phys.* **92**(1), 71–79.
40. E. V. Tkalya (2002) Spontaneous electric multipole emission in a condensed medium and toroidal moments. *Phys. Rev. A* **65**, 022504-1–022504-5.
41. T. B. Jones (1995) *Electromechanics of Particles*, Cambridge, New York.
42. S. Hirayama, H. Yasuda, M. Okamoto, and F. Tanaka (1991) Effect of pressure on the natural radiative lifetimes of anthracene derivatives in solution. *J. Phys. Chem.* **95**(8), 2971–2975.
43. Y.-P. Sun and M. A. Fox (1993) Fluorescence of 9-cyanoanthracene in supercritical ethane: A very unusual dependence of fluorescence lifetime on solvent refractive index. *J. Phys. Chem.* **97**(2), 282–283.
44. J. Saltiel, A. S. Waller, D. F. Sears, and C. Z. Garrett (1993) Fluorescence quantum yields of trans-stilbene-d_0 and -d_2 in n-hexane and n-tetradecane: Medium and deuterium isotope effects on decay process. *J. Phys. Chem.* **97**(11), 2516–2522.
45. J. K. Rice, E. D. Niemeyer, and F. V. Bright (1996) Solute-fluid coupling and energy dissipation in supercritical fluids: 9-cyanoanthracene in C2H6, CO2, and CF3H. *J. Phys. Chem.* **100**(20), 8499–8507.
46. S. Hirayama, K. Shobatake, and K. Tabayashi (1985) Lack of a heavy-atom effect on fluorescence lifetimes of 9-cyanoanthracene-rare gas clusters in a supersonic free jet. *Chem. Phys. Lett.* **121**(3), 228–232.
47. D. Toptygin and L. Brand (1993) Fluorescence decay of DPH in lipid membranes: Influence of the external refractive index. *Biophys. Chem.* **48**(2), 205–220.
48. D. Toptygin and L. Brand (1995) Determination of DPH order parameters in unoriented vesicles. *J. Fluoresc.* **5**(1), 39–50.
49. M. M. G. Krishna and N. Periasamy (1998) Fluorescence of organic dyes in lipid membranes: Site of solubilization and effects of viscosity and refractive index on lifetimes. *J. Fluoresc.* **8**(1), 81–91.
50. M. M. G. Krishna and N. Periasamy (1998) Orientational distribution of linear dye molecules in bilayer membrances. *Chem. Phys. Lett.* **298**(4–6), 359–367.
51. E. P. Petrov, J. V. Kruchenok, and A. N. Rubinov (1999) Effect of the external refractive index on fluorescence kinetics of perylene in human erythrocyte ghosts. *J. Fluoresc.* **9**(2), 111–121.
52. P. Lavallard, M. Rosenbauer, and T. Gacoin (1996) Influence of surrounding dielectrics on the spontaneous emission of sulforhodamine B molecules. *Phys. Rev. A* **54**(6), 5450–5453.
53. G. Lamouche, P. Lavallard, and T. Gacoin (1998). Spontaneous emission of dye molecules as a function of the surrounding dielectric medium. *J. Luminesc.* **76–77**, 662–665.
54. G. Lamouche, P. Lavallard, and T. Gacoin (1999) Optical properties of dye molecules as a function of the surrounding dielectric medium. *Phys. Rev. A* **59**(6), 4668–4674.
55. K. H. Drexhage (1970) Influence of a dielectric interface on fluorescence decay time. *J. Lumines.* **1,2**, 693–701.